SANDIA REPORT
SAND2024-12645
Printed September 2024

Sandia National Laboratories

Non-nuclear Component Signatures for Warhead Dismantlement Confirmation

Peter Marleau
Will Johnson
Hadar Lazar
Shiloh Sanchez
Elicia Tiano

Prepared by
Sandia National Laboratories
Albuquerque, New Mexico
87185 and Livermore,
California 94550

Issued by Sandia National Laboratories, operated for the United States Department of Energy by National Technology & Engineering Solutions of Sandia, LLC.

Available to DOE and DOE contractors from
U.S. Department of Energy
Office of Scientific and Technical Information
P.O. Box 62
Oak Ridge, TN 37831

Telephone: (865) 576-8401
Facsimile: (865) 576-5728
E-Mail: reports@osti.gov
Online ordering: http://www.osti.gov/scitech

Available to the public from
U.S. Department of Commerce
National Technical Information Service
5301 Shawnee Rd
Alexandria, VA 22312

Telephone: (800) 553-6847
Facsimile: (703) 605-6900
E-Mail: orders@ntis.gov
Online order: https://classic.ntis.gov/help/order-methods/

ABSTRACT

The verification of warhead dismantlement is expected to be an important component in future arms reduction treaties. Historic approaches developed with future arms control treaty verification in mind often involve intrusive measurements, process monitoring, and/or inspector presence to provide confidence that an authentic warhead has been dismantled. This work explores the possibility of reducing the negative impacts of these invasive approaches while also delivering a method that is more likely to provide non-sensitive data that can be shared with not only other nuclear weapons states but also non-nuclear weapons states partners.

This work explores a novel approach for verifying dispositioned non-nuclear weapon components, providing confidence post-dismantlement that a treaty accountable item that was dismantled was in fact a treaty-relevant nuclear weapon system as declared. This method provides an alternative to intrusive inspection processes in nuclear weapons production environments, which would require significant changes to the host's operational behaviors. It achieves this by identifying intrinsic neutron-induced signatures of non-nuclear components to determine their authenticity and estimate the duration they were exposed within a nuclear weapons system using technologies that are already in use for other national security applications. Intrinsic radiation effects studies are already a part of the stockpile aging and surveillance evaluations. However, none of these technologies and approaches have been previously considered for verification applications of non-nuclear component disposition.

In this report, we introduce modeling studies that have been used to identify the most promising candidate parts and materials with signatures that are measurable and actionable. These models have been validated with laboratory measurements of signatures induced by the exposure of candidate materials to neutrons over a range of times. Predictive modeling then demonstrates the methodology for estimating exposure times and/or limits. Laboratory measurements of authentic non-nuclear parts from a dismantled warhead demonstrate the feasibility of employing these signature measurements. And finally, a concept of operations (CONOPS) for the potential use of this methodology is presented.

CONTENTS

LIST OF FIGURES

LIST OF TABLES

This page left blank

1. INTRODUCTION

In anticipation of the impending termination of all U.S. nuclear arms control treaties in 2026, the focus of arms control research and development should now shift toward future treaties, which are anticipated to include accountancy on the scale of individual warheads. As of now, there are no accepted solutions for confirming the authenticity of a warhead nor its dismantlement that simultaneously provides sufficient confidence to the inspecting party of the treaty compliance and assurance to the host party that sensitive information is protected. An approach that avoids direct measurement of potentially sensitive information is therefore desirable.

This work investigates the use of signatures that have been imprinted in non-nuclear components to confirm warhead authenticity and that dismantlement has occurred. The intrinsic neutron radiation present in warheads gives rise to nuclear transmutation in the non-nuclear parts and materials. Differing transmutation cross-sections and activation product half-lives can be used in combination to provide bounds on service-life (exposure time) and dismantlement dates (cool-down period).

The presence of long-lived activation products is indicative of long-term inclusion in an assembled device, while short-lived spectator products can provide evidence that the parts were recently removed as a component of a warhead. Further, several common materials in these systems, such as stainless steel, have multiple activation products with differing decay constants. By measuring the ratios of decay gamma-ray emission rates from these materials, the duration of neutron exposure, and thus the lifetime within the warhead, can be confirmed.

In Section 3, we present the results of predictive modeling of measurable signatures from neutron activation for several common non-nuclear materials found in nuclear weapons systems. We observe growing line strengths over a period of years of neutron irradiation, demonstrating that it necessitates decades of exposure to converge to full strength, and thus validating spectroscopy as a probe to irradiation duration. As an analog to warhead verification scenarios, we then model the neutron exposure of non-nuclear components.

In Section 4.1, we validate these models by measuring the gamma-ray signatures of three different stainless-steel samples that were irradiated with a Californium-252 source over the course of six months. Spectral measurements were collected over a 24-hour period with a high-purity Germanium (HPGe) detector approximately every four weeks. We benchmark these results with simulations and demonstrate that the relative strengths of these lines reflect the time spent in proximity to the neutron source.

In Section 4.2, we present HPGe measurements of signatures obtained from authentic, non-nuclear parts from a dismantled warhead. This approach leverages processes that currently exist in host facilities rather than inserting intrusive inspection processes into the nuclear weapons production environment that would require changes in host operational behaviors. The majority of components in nuclear weapon systems are non-nuclear mechanical, structural, or electronic assemblies. The United States already has a disposition (demilitarization) process for all nuclear weapons parts; the methodologies and pathways for which are clearly defined. There are sensitivities surrounding the design of components that make up the nuclear package which preclude visual and physical access pre-disposition, and therefore limit options for verification. However, most non-nuclear components, hardware, and materials are commonly dispositioned into remnant forms which are then further disposed of in several ways, including: landfill, standard waste streams and commercial recycling processes. These processes could provide a bevy of verification opportunities while also protecting the sensitivity of design information.

2. APPROACH

When neutrons interact with atomic nuclei, they can be captured, resulting in the formation of new isotopes or elements characterized by long-lived excited states (1). The presence of these radionuclides can then be detected by the gamma-rays that are emitted at characteristic energies as they decay. In the context of nuclear warheads, the intrinsic neutron radiation (2) emitted by the nuclear material can cause this activation via neutron transmutation in the surrounding non-nuclear components.

Equation 1: The activity as a function of neutron exposure and cool-down time

$$A = N\sigma\phi(1 - e^{-\lambda t_a})e^{-\lambda t_w}$$

The activities of these metastable isotopes are given by Equation 1 in which σ is the neutron capture cross section, ϕ is the neutron flux, N is the number of target (parent) atoms, λ is the decay constant, t_e is the time exposed, and t_w is the time measured.

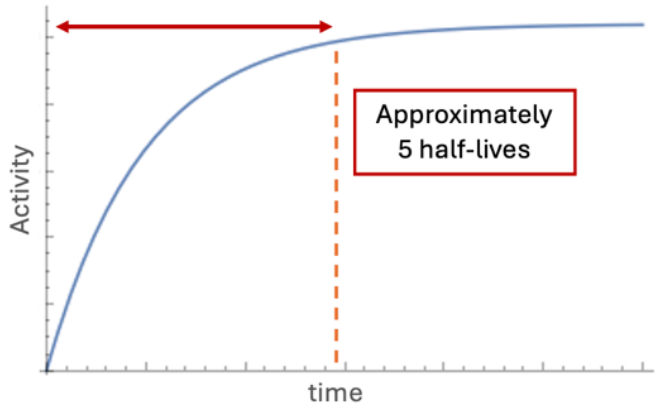

Figure 1: Illustration of the build up of a radionuclide as it is exposed to a neutron flux. Secular equilibrium is reached after approximately 5 half-lives.

The presence of radionuclides with longer lifetimes are indicative of decades-long exposure to nuclear material (visualized in Figure 1). Meanwhile, radionuclides with shorter timescales inform the length of time since exposure has concluded (also known as cool-down) and are therefore telling of the time since dismantlement.

The ratio of the activities of two radionuclides produced by the same neutron exposure on two different target atoms (shown in Equation 2) depends only on the ratio of the number of parent atoms exposed (R_N), which is dependent entirely on the material composition, the ratio of cross sections (R_σ), and the exposure and cool-down times. The neutron flux terms cancel out, rendering the neutron source irrelevant such that flux can vary throughout the volume of the exposed material without affecting the signature.

Equation 2: The ratio of activities for two radionuclides induced by the same neutron flux

$$R = R_N R_\sigma \frac{(1 - e^{-\lambda_2 t_a})e^{-(\lambda_2 - \lambda_1)t_w}}{(1 - e^{-\lambda_1 t_a})}$$

3. MODELING

We have developed modeling capabilities to estimate the energy-dependent intrinsic neutron radiation flux through any non-nuclear component in one of the US stockpile systems. This was used to estimate the expected neutron-induced transmutation within non-nuclear materials. We also developed the capability to estimate the expected gamma-ray emissions based on the materials present, length of exposure of this neutron flux, and the length of time since last exposure.

3.1. Signature Studies

These tools were first used to calculate the activities of the materials within various components with notional neutron source terms. This enabled the identification of several candidate isotopes in commonly used materials with signature strengths large enough to confirm that the non-nuclear components have been exposed for expected durations within uncertainties (or at least some minimum length of exposure), as well as the length of time since last exposure after dismantlement had occurred.

3.1.1. Modeling Chain

To model expected activation and subsequent decay and gamma emission, we used:

- GADRAS (3) to model the neutron production by a neutron source, as well as the transportation of neutrons through the moderating material surrounding the source. This provided an energy dependent neutron flux impinging onto materials of interest. GADRAS internally uses the SOURCES-4C and PARTISN codes to generate neutron source terms, and perform neutron transport, respectively.
- Several codes were used to model neutron interactions within different materials, including:
    - GEANT4 (4): The "Activation" sample code of Geant4 was adapted to detect activations, record which nuclides were made, and compute the expected production rates, for the nuclides. This code was used to compare against the irradiation measurements described in Section 4.1. The code for this stage of simulation can be found at (5).
    - Oak Ridge Isotope Generation Code (ORIGEN) (6): One use of this code is to find time dependent activation products by means of neutron transmutation, fission, and radioactive decay for a given sample with an input material definition and flux term. This was used as a second comparison for GEANT4 for the measurements described in Section 4.1.
    - *Periodictable* (2): This is a python package that provides expected neutron activation from time spent in a beam line. It only needs a formula of the material used, a flux, a mass, and an exposure time to compute activation on a sample, making it a good tool to use on first pass to find candidate materials.
- Custom code was written, on top of the SandiaDecay library (7), to model buildup and decay of the activation nuclides, using the rates derived in the previous step. This code also provides the expected gamma energies and intensities, taking into account decay during the measurement. Several alternative codes were evaluated for this task, but limitations prevented their use. The code for this stage of simulation can be found at (8).

- The output of the previous step was then either fed into GADRAS, using custom code to create 1DM files that GADRAS can ingest, to create predicted spectra, or it was used with custom code based off InterSpec (9) to determine expected detection limits. However, since we were unable to fully characterize the primary detector used for sample measurements, only approximate detector response function, or efficiency curves were able to be used for either of these tasks.

3.1.2. Component Materials and Masses

The material compositions and masses from eight candidate non-nuclear components from the U.S. Stockpile with a range of compositions were identified. Using the modeling code described in the previous section, we modeled neutron irradiation of each material to evaluate the expected signatures and determine the best candidates for future measurements. The material compositions, densities, and masses of the candidate components that were studied can be found in Table 1.

Table 1 – Materials, densities, and masses of several components that were modeled in this study

Component	Materials	Density (g/cc)	Min Mass (g)	Max Mass (g)
Comp_1	6061 Aluminium Alloy	2.7	5249	6416
	Alumina	3.97	6	7
	Epon 828	1.16	688	841
	304 Stainless Steel	8	80	97
Comp_2	6061 Aluminium Alloy	2.7	720	880
Comp_3	6061 Aluminium Alloy	2.7	64	78
	Aluminum Bronze	7.44	5	6
	Ceramic-Alumina	2.6	0.4	0.5
	304 Stainless Steel	8	533	652
	303 Stainless Steel	8	17	21
Comp_4	5052-H32 Aluminum	2.68	0.12	0.14
	Nickel	8.902	27	33
	Glass-Phenolic	1.94	0.02	0.03
	Silicone Rubber	1.45	0.007	0.009
	304 Stainless Steel	8	204	250
	465 Stainless Steel	7.86	1.6	2
	316 Stainless Steel	8	24	29
	416 Stainless Steel	7.8	30	37
Comp_5	Polyurathane Foam	0.1602	36	44

Component	Materials	Density (g/cc)	Min Mass (g)	Max Mass (g)
	6061 Aluminium Alloy	2.7	196	240
	7075 Aluminium Alloy	2.804	2306	2818
	Alumina	3.97	36	44
	Butyl-Rubber	0.92	1.2	1.4
	Nylon-66	1.314	4.5	5.5
	Peek	1.3	2	2
	Glass-Phenolic	1.94	83	102
	304 Stainless Steel	8	114	139
Comp_6	Glass-Phenolic	1.94		
	Polyurathane Foam	0.1602		
	6061 Aluminium Alloy	2.7		
	Alumina	3.97		
	Epon 828	1.16		
	Nylon	1.14		
	Glass-Phenolic	1.94		
	Polymide	1.4		
	304 Stainless Steel	8		
Comp_7	13-8PH Stainless Steel	7.8	95	116
	Copper	8.96	0	0
	Copper 102	8.94	10	12
	Diallyl-Phthalate w/o glass fiber	1.121	0	0
	Epon 828	1.16	0	0
	Epoxy	1.13	0	0
	Hiperco 50 Alloy	8.12	69	84
	Nitronic 60 Stainless Steel	7.62	2	2
	Silicon Nitride	3.44	7	9
	302 Stainless Steel	7.86	0	0
	304 Stainless Steel	8	451	551
	440C Stainless Steel	7.8	17	21

Component	Materials	Density (g/cc)	Min Mass (g)	Max Mass (g)
	Titanium Alloy	4.45	3	3
	Vespel SP1	1.43	0	0
Comp_8	6061 Aluminium Alloy	2.7	7276	8893
	Epon 828	1.16	2202	2691

3.1.3. Candidate Materials

In order to obtain a list of candidate material, each of the materials listed in Table 1 was modeled using the software described in Section 3.1.1. First, a general flux was assumed using an unclassified model of a polyethylene-reflected plutonium metal sphere (a.k.a. the BeRP ball) that is commonly used for subcritical neutron measurements (10). This yielded an incident neutron flux of 300 n/cm^2/s and a thermal/fast neutron ratio of 2 that was then put into the *periodictable* python package, standardized to a 1 gram mass. The results were then scaled to match the listed minimum mass. This was used as a starting point for the modeling with the realization that the results can be scaled according to any specific flux that is calculated in future modeling studies.

A minimum detectable activity was calculated using the Curie method at a 95% confidence interval for the most sensitive gamma-ray energy of the nuclide (interpreted as the strongest peak) assuming a 1-inch detector distance, an efficiency curve for a 40% HPGe, and 2.5 mm shielding of stainless steel. The backgrounds that were used in these calculations were measured at two detector locations. One background was collected from a 48-hour background measurement by a Canberra Germanium detector within a lead-lined low-background chamber taken in Livermore, California. Another was a 24-hour background measurement taken with a similar low-background detector in Albuquerque, New Mexico. Elevation makes a difference in the neutron background given the abundance of high energy neutrons at higher elevations from cosmic ray interactions in the atmosphere. These cosmic neutrons interact with the shielding material surrounding and germanium within detector to cause a elevation-dependent gamma-ray background. In the remainder of this report, we used the background file corresponding to the Livermore site, as that is the lower overall, but the higher background measurement can be used in future studies to scale to other elevations.

We then calculated how long after irradiation the expected activity decays such that it is below the minimum detectable activity. Components that produced radionuclides with activities that were significantly above the minimum detectable activity had interaction cross sections and enough material mass to be the promising radionuclides to study. Candidate materials decaying to these radionuclides were therefore our focus of study.

A list of nuclides of interest is compiled in Table 2 through Table 3. Table 2 lists those radionuclides with half-lives on the order of years, Table 3 list those with half-lives on the order of months, and Table 4 on the order of days to weeks. Those that were empirically determined to have high signal-to-noise are highlighted. Some of the most useful radionuclides with sensitivity to exposure times potentially similar to service lifetimes (i.e., years to decades) include Co-60, Sb-125, Mn-54, and Zn-65. Those that are most useful with sensitivity to exposures and/or cool-down periods of months include Sn-113, Sc-46, Co-58, Fe-59, and Cr-51, and those with sensitivity to cool-down periods

potentially similar to the time between dismantlement and verification measurements (i.e., days to weeks) include Sc-47, Mo-99, Cu-67, Na-24, Zn-69m, Cu-64, and K-42.

Of special significance, many of these nuclides are produced in the parent materials found in stainless steels. Table 5 lists those that can be found in many stainless-steel compositions. This is advantageous in that a single material could produce signatures that can provide confidence in both the length of exposure within a warhead, and the length of time since it has been removed from the warhead.

Table 2: List of radionuclides that were produced in the materials that were simulated with half-lives on the order of years. Only those that are highlighted are expected to have activities with a reasonable chance of detection in a low-background spectrometer.

Nuclide	Half-Life(days)	Half-Life (years)
Ni59	27759000	76000
Nb94	7414570	20299.99
Mo93	1461000	4000
Sn121m	16034.5	43.90007
Nb93m	5891.48	16.12999
Co60	1925.28	5.271129
Sb125	1007.56	2.758549
Fe55	1002.25	2.744011
Mn54	312.05	0.854346
Sn119m	293.1	0.802464
Zn65	243.931	0.667847

Table 3: List of radionuclides that were produced in the materials that were simulated with half-lives on the order of months. Only those that are highlighted are expected to have activities with a reasonable chance of detection in a low-background spectrometer.

Nuclide	Half-Life(days)
Sn123	129.2
Sn113	115.09
Sc46	83.79
Co58	70.86
Zr95	64.0319
Fe59	44.495
Cr51	27.701

Table 4: List of radionuclides that were produced in the materials that were simulated with half-lives on the order of days to weeks. Only those that are highlighted are expected to have activities with a reasonable chance of detection in a low-background spectrometer.

Nuclide	Half-Life(days)
Sn117m	13.76
Nb92m	10.15
Sn125	9.64
Sc47	3.3492

Mo99	2.7475
Cu67	2.57625
Sc48	1.81958
Ni57	1.48333
Nb96	0.972917
Zr97	0.697875
Na24	0.624875
Zn69m	0.573333
Cu64	0.529208
K42	0.515

Table 5: List of the most useful radionuclides produced in stainless steels

Nuclide	Half-Life (years/days)
Co-60	5.271 / 1,925.2
Sb-125	2.759 / 1,007.7
Mn-54	0.854 / 311.9
Zn-65	0.668 / 244.0
Co-58m	0.194 / 70.9
Cr-51	0.076 / 27.8

3.2. Predictive Modeling

Measurements of the ratios of activities between radionuclides are promising because they are independent of neutron flux, and thus require no information on the location or orientation of a component in the warhead. The ratios of activities of radionuclides of different half-lives depends only on the material composition, as shown in Equation 2, and provide information on the duration of the service-life, as they converge after different lengths of times. Analytical examples of some of the most useful ratio combinations that can be obtained from stainless steel are shown in Figure 2.

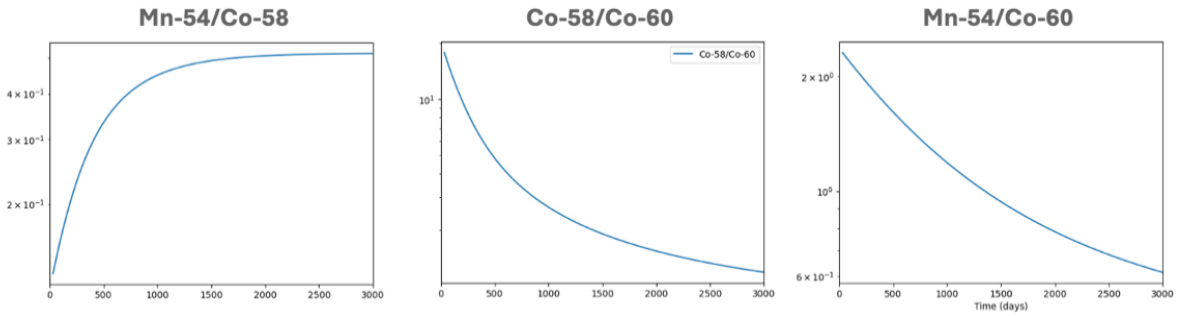

Figure 2: Analytic trends of activity ratios for a some of the radionuclides produced in stainless steels

Tracking multiple ratios, each providing a different exposure time estimates as a result of their different half-lives, can therefore constrain the total exposure of service-life. Moreover, it is

implausible to synthesize these signatures as they require specific decades-long exposures to obtain, and cannot be generated by shorter-duration, higher-flux exposures.

4. MEASUREMENTS

4.1. Validation

To build confidence around the tools we have developed and thus the conclusions they reap, we benchmarked them against a carefully controlled irradiation experiment. Three 120 grams stainless steel samples of a well-characterized composition (SAE 405, SAE 201, and 17Cr-9Ni [C1153a] shown in Table 6) were obtained and placed around a polyethylene shell with a thickness of 7 cm and inner void radius of 3 cm to moderate the neutron flux. Two Cf-252 neutron sources with a total activity of 0.32 mCi were positioned at the center of the shell (see Figure 3). The entire setup underwent irradiation inside a low-background over-container for a duration of 7 months. On a monthly basis, the disks were temporarily removed, and gamma-ray spectra were collected by a HPGe detector, Canberra GR2018.

Table 6: Material compositions of the three stainless steel disks used in this study.

Element	Mass Percentage (%)		
	SAE 405	SAE 201	17Cr-9Ni (C1153a)
Iron	85.1437	69.3757	71.947
Carbon	0.027	0.066	0.225
Chromium	13.52	16.69	16.7
Cobalt	0.02	0.127	0.127
Copper	0.26	0.442	0.226
Lead			0.006
Manganese	0.387	7.11	0.544
Molybdenum	0.023	0.331	0.24
Nickel	0.194	5.34	8.76
Phosphorus	0.022	0.038	0.03
Silicon	0.321	0.397	1
Sulfur	0.0003	0.0033	0.019
Vanadium	0.082	0.08	0.176

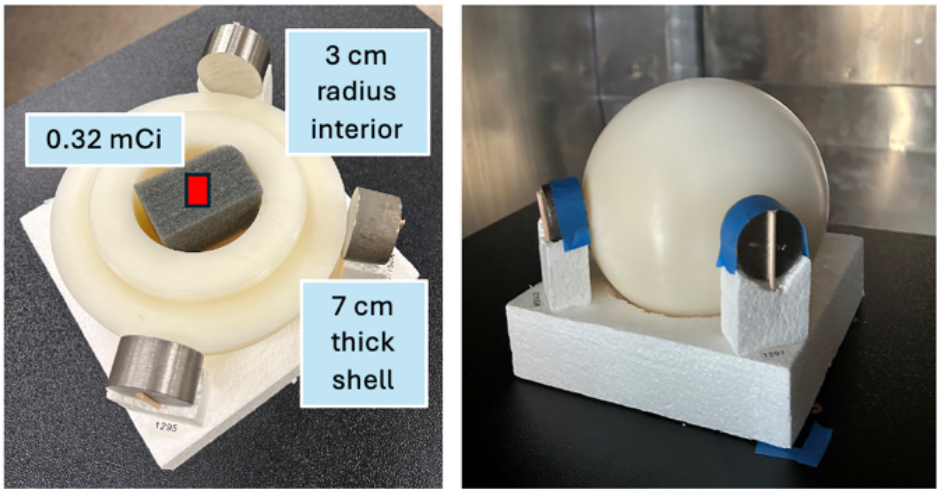

Figure 3: Measurement setup

The measurements revealed an ingrowth of radionuclide activities anticipated by the composition of each disk. These activities were calculated by fitting a relative efficiency curve to line energies using InterSpec (9). Figure 4 provides a spectrum and its relative efficiency analysis as an example.

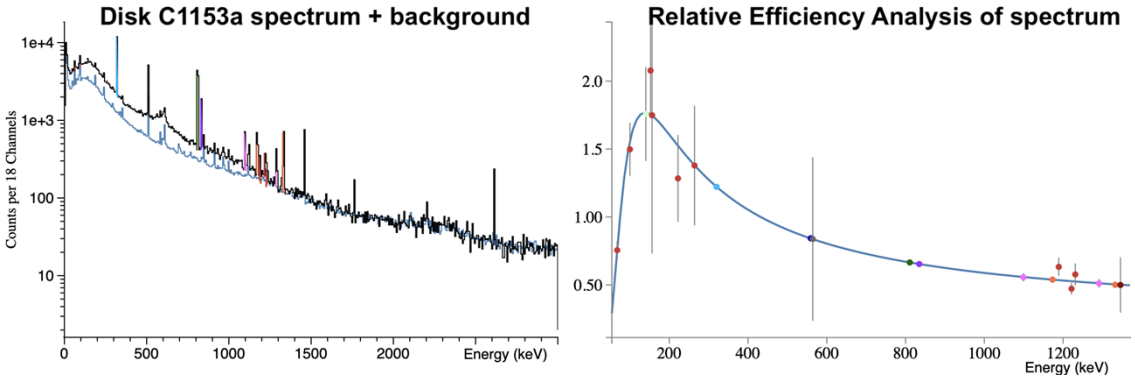

Figure 4: HPGe spectrum of the stainless steel disk and background (left), and results of the relative efficiency analysis (right).

This setup was reproduced in the Oak Ridge Isotope Generation Code (ORIGEN SCALE) (6), a tool for the calculation of time-dependent activities and radiation source terms for isotopes simultaneously generated or depleted by neutron transmutation, fission, and radioactive decay. A full description of the modeling is provided in Section 4.1.1. It was also modeled by our custom GEANT4+GADRAS codebase described in Section 3.1.1.

Table 7: 5th Measurement and corresponding prediction for 17Cr-9Ni (C1153a)

Nuclide	Relative Activity	Mass Fraction	Activity normalized	Data Uncertainty	Predicted Norm Act (GEANT4)	n-sigma away	Predicted Norm Activity (SCALE)	n-sigma away
Cr51	81093	0.2951	1.000000	0.11	1.000000	0.000000	1.000000	0.000000
Cu64	17022	0.001485	0.209907	0.404	0.003159	-1.954271	0.058058	-1.435339
Co58	11070	0.1172	0.136510	0.0847	0.276557	5.554473	0.211872	2.988966

Mn54	2237	0.09712	0.027586	0.0854	0.049345	4.254498	0.042083	2.834699
Fe59	1500	0.01014	0.018497	0.074	0.022036	1.099546	0.020276	0.552721
Co60	1333	0.3968	0.016438	0.0751	0.023298	2.383536	0.023299	2.383665
Mo99	205.4	0.0001439	0.002533	0.203	0.002066	-0.608305	0.004730	2.862619
As76 (uncertified)	104.7	0.00002242	0.001291	0.116	0.001580	1.036396	0.007148	21.001608
Sb122 (uncertified)	92.74	0.00007941	0.001144	0.697	0.001539	0.433876	0.002603	1.601612

Table 8: 5th Measurement and corresponding prediction for SAE 405

Nuclide	Relative Activity	Mass Fraction	Activity normalized	Data Uncertainty	Predicted Norm Act (GEANT4)	n-sigma away	Predicted Norm Activity (SCALE)	n-sigma away
Cr51	61798	0.49	1.000000	0.12	1.000000	0.000000	1.000000	0.000000
Mn54	2789	0.26	0.045131	0.07	0.069618	3.256711	0.062127	2.260447
Fe59	2331	0.03	0.037720	0.11	0.032077	-0.729796	0.028819	-1.151067
Co60	316.9	0.21	0.005128	0.15	0.004483	-0.509024	0.004603	-0.414102
Co58	239.8	0.01	0.003880	0.12	0.007217	3.838889	0.005821	2.232395
As76 (uncertified)	198.4	0.00	0.003210	0.24	0.003044	-0.153439	0.007454	3.922345
Sb122 (uncertified)	98.16	0.00	0.001588	0.29	0.002342	1.225224	0.003151	2.542657

Table 9: 5th Measurement and corresponding prediction for SAE 201

Nuclide	Relative Activity	Mass Fraction	Activity normalized	Data Uncertainty	Predicted Norm Act (GEANT4)	n-sigma away	Predicted Norm Activity (SCALE)	n-sigma away
Mn56	77796	0.00	1.000000	0.09	1.000000	0.000000	1.000000	0.000000
Cr51	66057	0.29	0.849105	0.07	0.778772	-0.491878	0.11600	-5.126993
Co58	5479	0.07	0.070428	0.09	0.135871	4.926958	0.01540	-4.142822
Mn54	1929	0.10	0.024796	0.09	0.038181	2.792760	0.0049500	-4.140548
Co60	1450	0.52	0.018638	0.11	0.017371	-0.319318	0.002670	-4.022291
Fe59	1447	0.01	0.018600	0.11	0.016092	-0.630147	0.002230	-4.112650
Tc99m	1156	0.0001	0.014859	0.26	0.008553	-1.165969	0.000611	-2.634289
W187 (uncertified)	323	0.0002	0.004152	0.07	0.015780	16.483599	0.002830	-1.873936
As76 (uncertified)	265.5	0.0001	0.003413	0.21	0.003026	-0.368271	0.0005504	-2.719703
Sb122 (uncertified)	68.91	0.0001	0.000886	0.52	0.001346	0.838158	0.000200	-1.248726

Table 7 through Table 9 exemplify how the measurements and predicted activities are in relatively good agreement. An additional systematic uncertainty of 10 percent was used for the real data in the n-sigma determination to account for the variation of the scaled activities depending on the

uncertainty in the fit of the detector's relative efficiency curve. It is expected that when the detector is characterized, activities and uncertainties will be better evaluated.

To validate the predicted buildup of radionuclide activities as a function of exposure time, we compare the measured relative activities of Mn-54 to Co-58 to modeled predictions for the 17Cr-9Ni stainless-steel disk in Figure 5. It can be seen that the predictions match the experimentally determined ratios within measurement uncertainties.

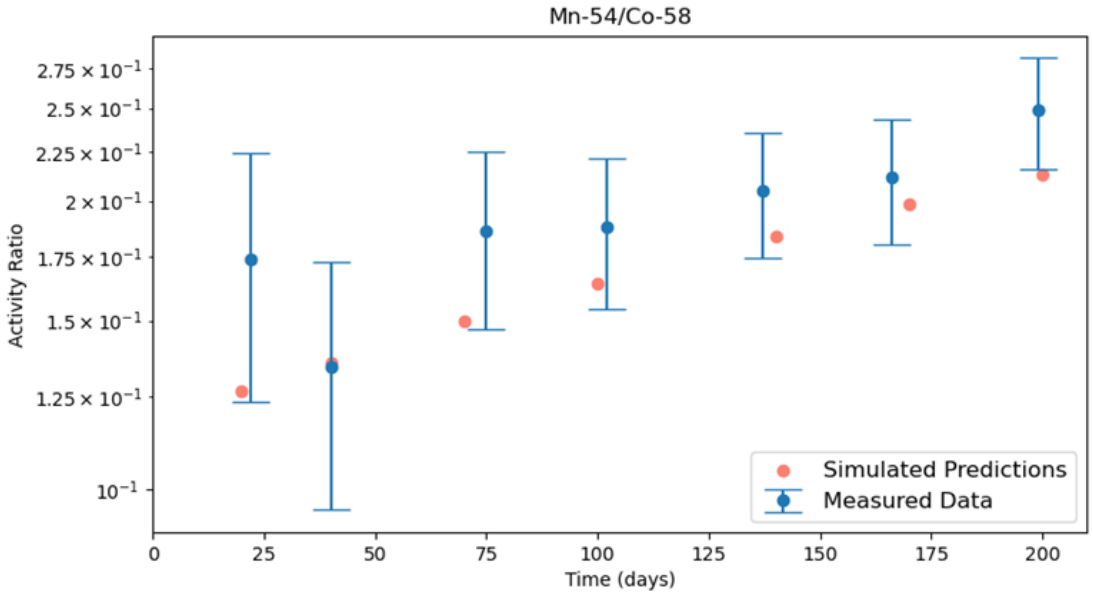

Figure 5: Measured and GEANT4 simulated ratios of Mn-54 to Co-58 activities for the 17Cr-9Ni (C1153a) disk as a function of exposure time.

Next, we sought to validate the method for using activity ratios to estimate the exposure time of an irradiated component. We produced analytic trends for the stainless-steel sample (see blue line in Figure 6) and compared them to the 137-day measurement of the stainless-steel data (green line). The measured activity ratios closely match the predicted activity ratios at the true exposure time of the measurement (orange dashed line). The black dashed lines display the predicted exposure time uncertainty range. Table 10 through Table 12 provide the measured ratios for each sample.

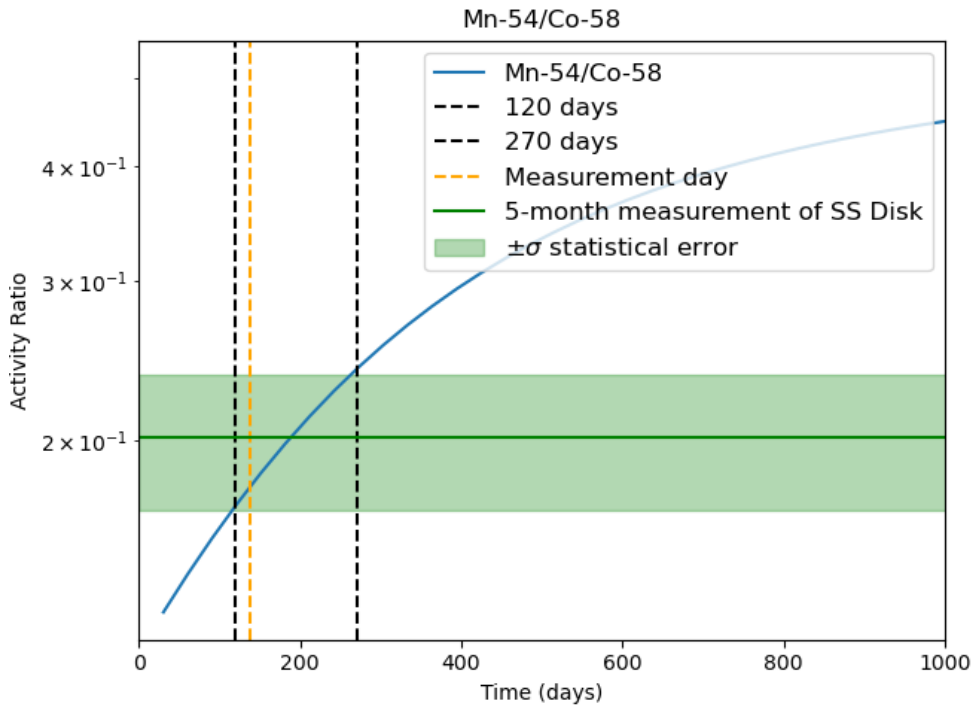

Figure 6: Measured activity ratio compared to analytic trend for the 17Cr-9Ni (C1153a) disk

Table 10: Measured activity ratios for the 137-day exposure of the 17Cr-9Ni (C1153a) sample, seen in Figure 5.

Mn-54/Co-60	Mn-54/Co-58	Co58/Co60
1.6782	0.2021	8.3046

Table 11: Measured activity ratios for the 137-day exposure of the SAE 201 sample

Mn-54/Co-60	Mn-54/Co-58	Co58/Co60
1.6687	0.3527	4.7396

Table 12: Measured activity ratios for the 137-day exposure of the SAE 405 sample

Mn-54/Co-60	Mn-54/Co-58	Co58/Co60
3.2284	0.1492	23.7469

We also desired to gain an understanding of how long into a component's exposure could activity ratios continue to predict an exposure time range. For this reason, we propagated the disk's expected activity and measurement uncertainties to identify the maximum exposure for which an upper bound can be estimated (see **Figure** 7). We found that the ratios generate an exposure time estimate for at least 6500 days (17.8 years), after which they only provide a minimum exposure time. When statistical errors are improved—which could be done by increasing measurement time, measuring more material, and characterizing the detector response better—the minimum exposure time will likewise increase.

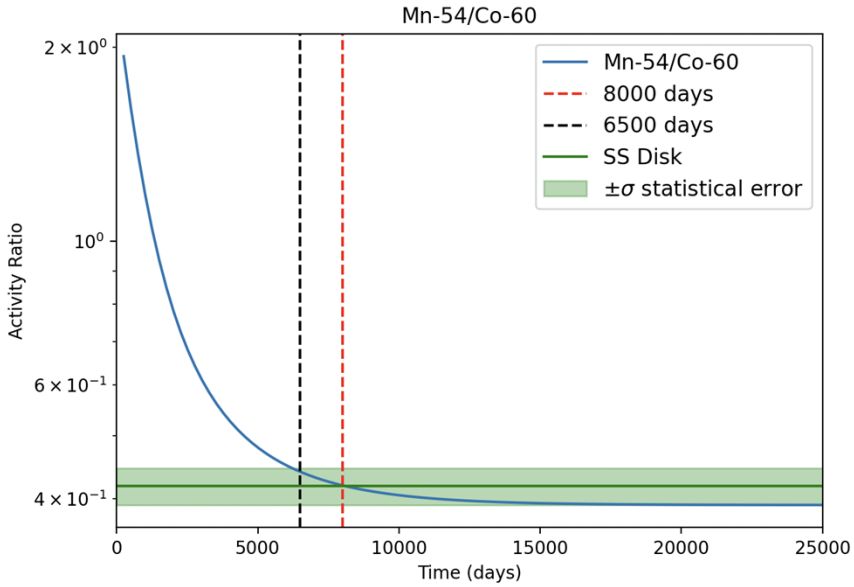

Figure 7: Propagated activity ratio of measurement compared to a long-term analytic trend.

4.1.1. ORIGEN Modeling

To validate the custom software chain described in the previous section, we applied a module of SCALE called MAVRIC, a 3-D Monte Carlo code traditionally used for shielding applications. This was used to model the component geometry and source term of the irradiated geometry. This enabled us to tally the neutron fluxes irradiating each component. Figure 8 below shows a 3D render of the set-up; the figure description cites the materials in the model's legend. There are some liberties taken with this model including the assumption that the Cf-252 source was embedded in a small solid sphere of stainless steel 304 0.1 cm thick, rather than two separate cylindrical encased sources, with a total neutron strength of 1183253 n/s assuming a neutron yield of 4.4e9 n/s per Ci of Cf-252 from spontaneous fission. This is equivalent to the assumed combined source strength the day of the 5th measurement.

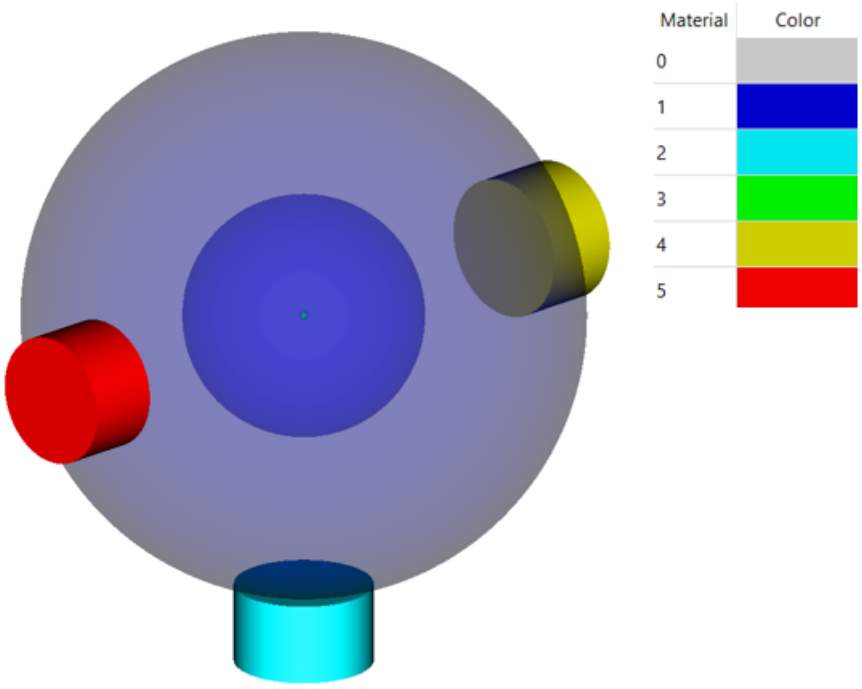

Figure 8: A model of the irradiation set-up shown in Figure 3. The legend of materials are: 0 – Void, 1 – HDPE, 2 – SAE405, 3 – SS304, 4 – SAE405, 5 – Disk C1153A.

A tally to find the flux through each of the samples using this model, along with the material definitions and masses, was then input into the Oak Ridge Isotope Generation Code (ORIGEN (6)) to obtain the expected activities. The ratio of predicted activities are shown in Table 7, Table 8, and Table 9 for each disk.

4.2. Non-nuclear Parts

We identified an opportunity to measure a non-nuclear part, a bracket composed of stainless steel (seen in Figure 9), that had relatively recently been removed from a nuclear weapon. Of the expected signatures, the isotopes Co-60, Co-58, and Mn-54, were positively detected, providing preliminary validation of this method experimentally (Figure 10).

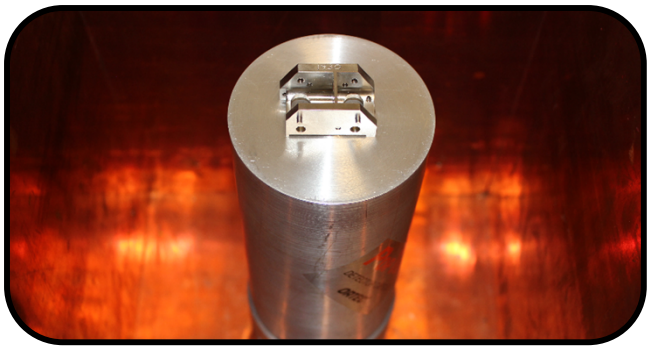

Figure 9: A dispositioned bracket on the HPGe spectrometer in low-background shield

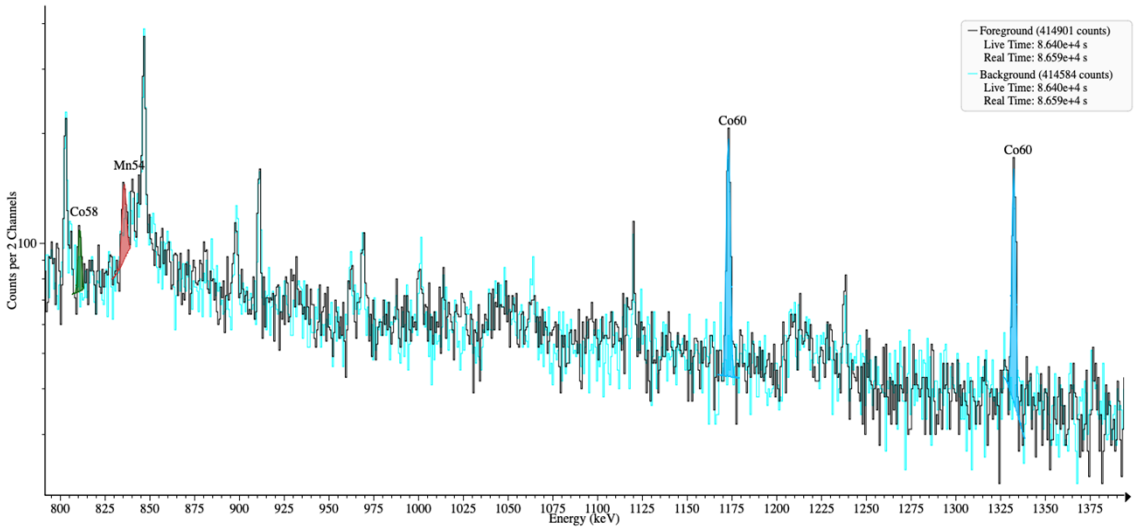

Figure 10: Measured spectrum of the bracket with labeled radionuclides

Two methods were used to calculate the activities of this bracket in InterSpec, first by (1) fitting a low-order relative efficiency curve, and by (2) adapting a standard Germanium detector response. The high systematic uncertainty for both methods is expected to improve when utilizing the specific detector response for this detector. For the time being, our measured range covers the statistical errors produced by both methods. Figure 11 compares this measured activity ratio range to the analytic trend produced for the stainless-steel disk with the most closely matched composition to that of bracket. The measurements were corrected for the cool-down period defined by the known dismantlement date. We demonstrate that the component must have been irradiated for at least a decade in order to produce results in this range. This result establishes the validity of this method to confirm a long-term service-life.

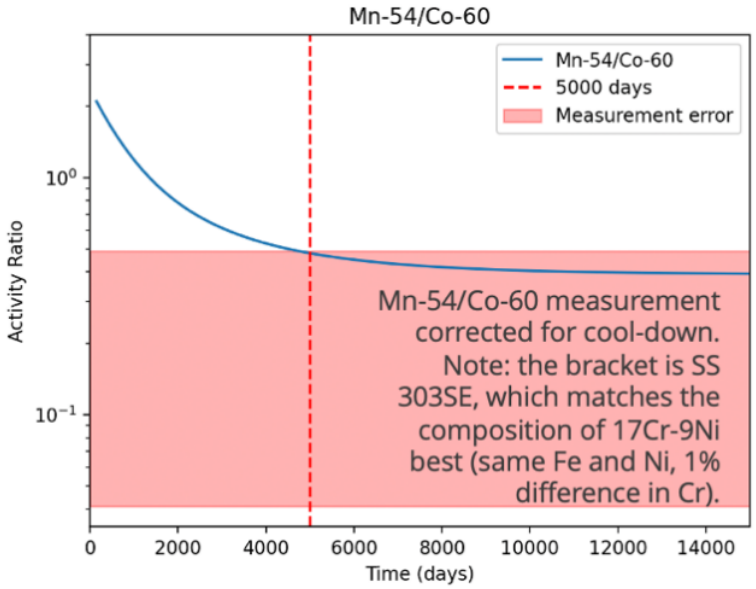

Figure 11: Measured activity ratios for the stainless steel bracket compared to the analytic trends of the stainless steel disk

For the measurements, the two methods produced the ratios before cool-down corrections listed in Table 13 and Table 14.

Table 13: Ratio measurements for the bracket using relative efficiency curve.

Relative Efficiency Curve:

Mn-54/Co-60	Mn-54/Co-58	Co58/Co60
0.10 (~±0.04 stat.)	0.69 (~±0.3 stat.)	0.15 (~±0.06 stat.)

Table 14: Ratio measurements for the bracket using the standard Ge detector response.

Standard Detector Response:

Mn-54/Co-60	Mn-54/Co-58	Co58/Co60
0.28 (~±0.16 stat.)	1.2 (~±0.78 stat.)	0.23 (~± -0.05 stat.)

5. CONOPS

5.1. Information Sensitivity

Information pertaining to the elemental/isotopic makeups of materials, such as common chemical compounds, polymers, families and grades of metals and their alloys, and their mass densities were gathered and approved for release for this study based on existing modeling and simulation studies of non-nuclear component parts. To avoid any risk that divulging composition information for specific parts could reveal component functionality for a particular nuclear weapon system we have not associated any material with any specific component or nuclear weapon system. Furthermore, a range of masses for these materials was provided rather than specific masses.

It was hypothesized that a range of spectral neutron flux values impinging on a range of non-nuclear components might be shareable, but we did not pursue it further as the radionuclide activity ratio method that we developed does not depend on knowledge of this flux.

5.2. Verification Measurements

After consultation with staff at the Pantex Plant, the project team developed a concept of operations that could be implemented within the normal conduct of operations at a nuclear facility. The disposition process for dismantled parts naturally segregates the different material compositions. Depending on the nature of the component, it could be sent directly to recycling or landfill, or undergo a process to remove any potentially sensitive design information. For example, some parts could be shredded until their geometries can't be inferred.

In the best-case scenario, entire non-nuclear parts could be tracked out of dismantlement with chain-of-custody (CoC) measures and turned over to a treaty partner entirely for confirmation measurements. Some parts, such as bolts, screws, or the bracket that was measured in Section 0 fit into this category.

Alternatively, if CoC could be maintained through the disposition process until the point that the non-nuclear components are shredded materials, then a potentially large mass of material could be released to a treaty partner for confirmation measurements.

In either case, it is not necessary to have prior knowledge of the absolute neutron flux to which the materials had been exposed. Further, the materials could have been from several parts that received a large range of neutron flux. This only affects the overall strength of the signature to be measured, but the ratio of radionuclide activities depends only on the initial composition and the efficiency for each production mechanism.

The anticipated CONOPS would therefore entail CoC measures that maintains the provenance of the parts and materials from the outputs of a warhead dismantlement process until a measurement can take place. Given the long half-lives of the radionuclides of interest, the delay between dismantlement and confirmation measurements could be weeks to months, as demonstrated in our own measurement of the bracket, and the length of that cool-down period can also be verified.

6. SUMMARY AND FUTURE WORK

By generating models of neutron transmutation by exposure to a neutron source, the most optimal non-nuclear component materials with observable gamma-ray signatures were identified. Our models also identified radionuclides that relay information on components' long-term neutron exposure and following cooling period. The ratios of activities of these radionuclides provide estimates on service-life.

Predictive tools were validated with measurements of irradiated, well-characterized stainless-steel samples. A measurement of a non-nuclear part was obtained, with preparations for additional non-nuclear component measurements underway. These promising preliminary results introduce non-nuclear disposition measurements as a potential option for non-intrusive verification, which may be integral in future arms control reduction treaties.

Correspondence with staff at Pantex has generated interest in pursuing similar measurements in the future. It was not able to be arranged before the close of this project, but arrangements were being planned for dispositioned materials to be released to us for measurement. Arrangements were also being made for the shipment and use of our newly acquired Fulcrum-40h HPGe spectrometer with low-background lead shield for measurements at the Pantex site.

Future work also includes creating higher fidelity models with exact geometries and spatially dependent flux values to determine activation products more accurately from the stockpile components. This would be an improvement on the preliminary study, as possible impacts of specifying geometry (such as self-shielding) and a finer neutron group structure on the flux would provide more precise predictions for this type of analysis.

REFERENCES

1. **Knoll, G.F.** *Radiation Detection and Measurement.* 4th. Hoboken : Wiley, 2010.
2. **Kienzle, Paul et. al.** PeriodicTable. *GitHub.* [Online] https://github.com/pkienzle/periodictable.
3. **Steven M. Horne, Gregory G. Thoreson, Lisa A. Theisen, Dean J. Mitchell, Lee T. Harding, Sean E. O'Brien.** *GADRAS Version 18 User's Manual.* 2019. SAND2019-14305.
4. *Geant4—a simulation toolkit.* **Agostinelli, S. et. al.** 3, s.l. : Nuclear Instruments and Methods in Physics Research Section A: Accelerators, Spectrometers, Detectors and Associated Equipment, Vol. 506. ISSN 0168-9002.
5. **Johnson, Will.** nonnucgeantsampleactivation. [Online] https://cee-gitlab.sandia.gov/wcjohns/nonnucgeantsampleactivation.
6. **W. Wieselquist, S. Hart, K. Bledsoe, S. Skutnik, K. Bekar.** *ORIGEN SCALE (Version 6.3).*
7. **Johnson, Will.** SandiaDecay. *GitHub.* [Online] https://github.com/sandialabs/SandiaDecay.
8. —. nonnucbuildupcalc. [Online] https://cee-gitlab.sandia.gov/wcjohns/nonnucbuildupcalc .
9. —. Interspec (v 1.0.12). *Github.* [Online] https://github.com/sandialabs/Interspec.
10. **Mattingly, John K.** *Polyethylene-reflected plutonium metal sphere : subcritical neutron and gamma measurements.* Sandia National Laboratories. 2009. SAND2009-5804.

DISTRIBUTION

Email—Internal

Name	Org.	Sandia Email Address
Technical Library	1911	sanddocs@sandia.gov

Email—External

Name	Company Email Address	Company Name

Hardcopy—Internal

Number of Copies	Name	Org.	Mailstop

Hardcopy—External

Number of Copies	Name	Company Name and Company Mailing Address

This page left blank

Sandia National Laboratories

Sandia National Laboratories is a multimission laboratory managed and operated by National Technology & Engineering Solutions of Sandia LLC, a wholly owned subsidiary of Honeywell International Inc. for the U.S. Department of Energy's National Nuclear Security Administration under contract DE-NA0003525.